Active species in N2 flowing post-discharges

André Ricard, A. de Souza

Classification
Physics Abstracts
52.80 — 52.70

Active species in N_2 flowing post-discharges

A. Ricard ([1]) and A. R. de Souza ([2])

([1]) LPGP, Bât. 212, CNRS, Université Paris-Sud, 91405 Orsay, France
([2]) Depto. de Fisica, UFSC, 88.000, Florianopolis, SC, Brazil

(Received 3 December 1993, revised 27 April 1994 and 20 July 1994, accepted 1 September 1994)

Abstract. — The afterglow in D.C. and H.F. N_2 flowing discharges has been analysed by emission spectroscopy. Production of excited species has been studied in conditions of late $\Delta t = (1-5) \times 10^{-1}$ s and early $\Delta t = (0.5\text{-}5) \times 10^{-2}$ s afterglows. The late afterglow is characterized by the N_2 1st positive emission with a strong enhancement of the $N_2(B, v' = 11)$ level compared to the other $N_2(B, v')$ levels which is a signature of N atom density. By NO titration, we have determined that N/N_2 dissociation degrees are respectively 4.1 % and 2.7 % in a 60 W H.F. and in a 50 mA D.C. post-discharge at 4.5 Torr. The early afterglow is characterized by a strong 1st positive emission which has been analysed from the $N_2(A) + N_2(X, v > 5)$ excitation transfer reaction. By introducing a little $CH_4(10^{-4}\text{-}10^{-3})$ or $H_2(10^{-2}\ 10^{-1})$ into the N_2 D.C. and H.F. post-discharges, $N_2(A)$ quenching rates have been obtained indicating that the $N_2(A)$ is only excited on the two first vibrational states in the early afterglows.

1. Introduction.

Production of active species in a flowing post-discharge is studied in connection with plasma reactions for surface treatment. With N_2 D.C. and microwave discharges, the N-atom flux in the post-discharge has been previously determined by NO titration and has been correlated to the growing of iron nitrided layers [1]. The post-discharge with N atoms is characterized by a specific yellow afterglow [2], following the reaction :

$$N + N + M_2 \rightarrow N_2(B, 11) + M_2 \qquad \text{(a)}$$

$$N_2(B, 11) \rightarrow N_2(A, 7) + h\nu\,(580\ \text{nm})\,.$$

The strong enhancement of emission from $N_2(B, 11)$ state compared to that of other $N_2(B, v')$ levels is the signature of N atoms in the post-discharges which can be easily observed for gas pressures greater than 1 Torr (three body reaction) and for times greater than 0.1 s (late afterglow).

At shorter times and gas pressure 0.1-1 Torr in the post-discharge, other active species such as $N_2(A)$ metastable molecules are still sufficiently numerous to produce specific reactions.

It is the purpose of the present paper to report the results of the emission spectroscopy in the late and early N_2 afterglows. The comparison of N-atom production has been realized between D.C. and microwave discharges. The effect on the N_2 excited states of adding small CH_4 and H_2 percentages to N_2 is specifically studied.

2. The experimental set-up.

The experimental set-up is reproduced in figure 1. Several discharge configurations have been arranged in pyrex tubes of diameters 2 cm and 0.4 cm.

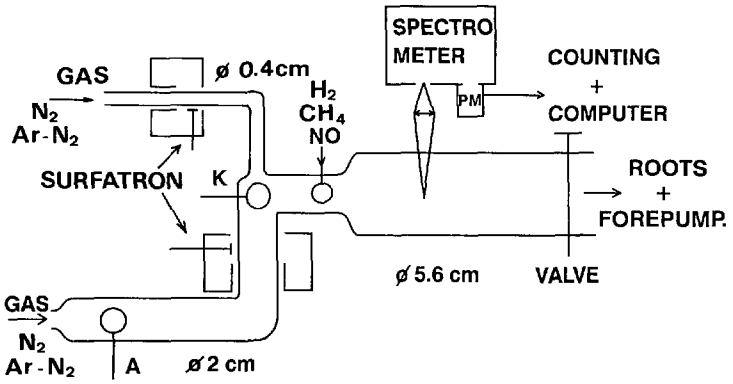

Fig. 1. — D.C. and H.F. flowing discharges and post-discharge. (A) anode, (K) cathode.

A positive column can be produced between side-armed anode (A) and cathode (K) 30 cm apart along the tube of diameter 2 cm. Microwave discharges can be independently produced in tubes of diameter 2 cm and 0.4 cm, by using a surfatron launcher [3]. The tube diameters have been chosen to allow the comparison with previous results in D.C. (diameter 2 cm) and in microwave (0.4 cm) N_2 post-discharge reactors [1]. In the experimental set-up of figure 1, the NO gas can be introduced at the beginning of the post-discharge tube for N-atom titration. The post-discharge tube of diameter 5.6 cm is connected to a 400 m^3/h Roots pump system by means of a throttle valve. The gas pressure and flow-rates are measured with an absolute gauge and mass flowmeter controls, respectively :

The residence time (Δt) in the post-discharge is deduced from the values of gas pressure (p) and standard flow rate (Q_0) at room gas temperature (300 K) : $\Delta t = \pi R^2 \frac{Z}{Q_0} \frac{p_0}{p}$ where R is the tube radius, Z distance between the discharge end and the observation area and p_0 the atmospheric gas pressure.

The afterglow is analysed by emission spectroscopy using a Jobin-Yvon HR640 spectrometer equipped with a 1 200 grooves per mm diffraction grating and a Hamamatsu R928 photomultiplier, connected to a photon counting and a computer controling system.

3. Production of N atoms in the late afterglow : $\Delta t = (1\text{-}5) \times 10^{-1}$ s.

In conditions of N_2 or Ar-N_2 late afterglow, the 1st positive emission has been recorded and is reproduced in figure 2 for a H.F. (60 W, dia. 0.4 cm) Ar-10 % N_2, post-discharge at 4.5 Torr and a time of $\Delta t = 0.3$ s. By introducing NO into the post-discharge, the N_2 dissociation

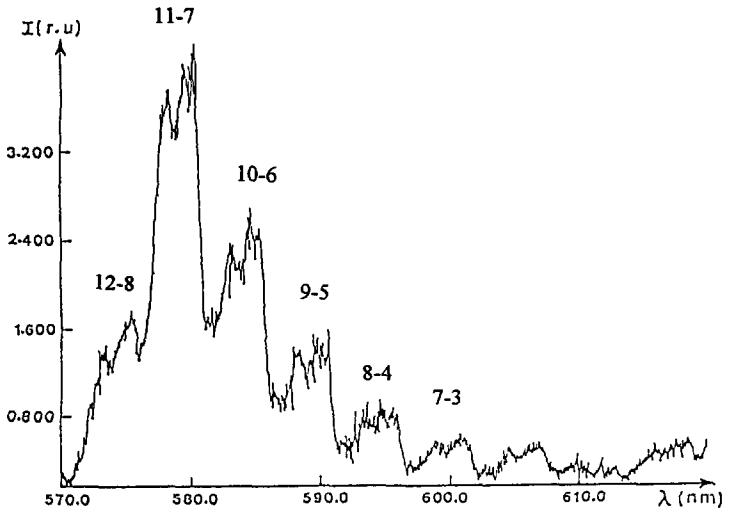

Fig. 2. — N_2, 1st pos. intensity in Ar-10 % N_2, H.F. (60 W, dia. 0.4 cm) post-discharge at p = 4.5 Torr and time Δt = 0.3 s (late afterglow).

degree which is obtained after extinction of NO_β bands and before the NO_2 continuum appears [1, 2] has been determined at the null point.

It has been found $\frac{[N]}{[N_2]} = 2.7$ % in the D.C. Ar-10 % N_2 post-discharge at 4.5 Torr and 50 mA in the positive column (R = 1 cm) where the electric field and the power can be estimated to be 50 V/cm^{-1} [4] and 75 W, respectively. With the H.F. 1 000 MHz Ar-10 % N_2 discharges at 4.5 Torr and 60 W, the dissociation degree is higher : $\frac{[N]}{[N_2]} = 4.1$ and 4.3 % after the discharge tubes of diameter 2 cm and 0.4 cm.

The uncertainty of N-atom density measured by NO titration is about 20 %. The gas pressure is limited to about 5 Torr in the present post-discharge tube (dia. 5.6 cm). In these conditions, the CN-violet band emissions were not detected when a little CH_4 (10^{-4}-10^{-3}) was added to the N_2 and Ar-N_2 post-discharges as previously reported [5]. The CN emission results from C + N recombination reactions, the carbon atoms are produced either by olefins in impurity [5] or by introduction of 10^{-3}-10^{-4} CH_4 into N_2 [6] in HF post-discharges, for pressures in the range 10-100 Torr.

In the present Ar-N_2 H.F. post-discharge at 4.5 Torr, 60 W, the pink afterglow is observed at time $\Delta t = 10^{-1}$ s, just before the late afterglow. The pink afterglow is characterized by a strong intensity of N_2^+ first negative bands as analysed in reference [7]. At shorter times $\Delta t = 10^{-2}$ s in the case of the 4.5 Torr post-discharge, the early afterglow is characterized by strong intensity of the N_2 first positive bands without N_2^+ first negative emission. Such an early afterglow is observed alone with a strong intensity at low gas pressures (0.2-0.5 Torr) and short residence times (5×10^{-3}-5×10^{-2} s).

4. Active species in the early afterglow : $\Delta t = (0.5\text{-}5) \times 10^{-2}$ s.

The first positive emission in the Ar-10 % N_2 early afterglow of the H.F. discharge (dia. 0.4 cm, $\Delta t = 2 \times 10^{-2}$ s, p = 0.4 Torr) is reproduced in figure 3 for the same spectral range as in figure 2. By comparing with the spectrum in the late afterglow (Fig. 2), it can be observed

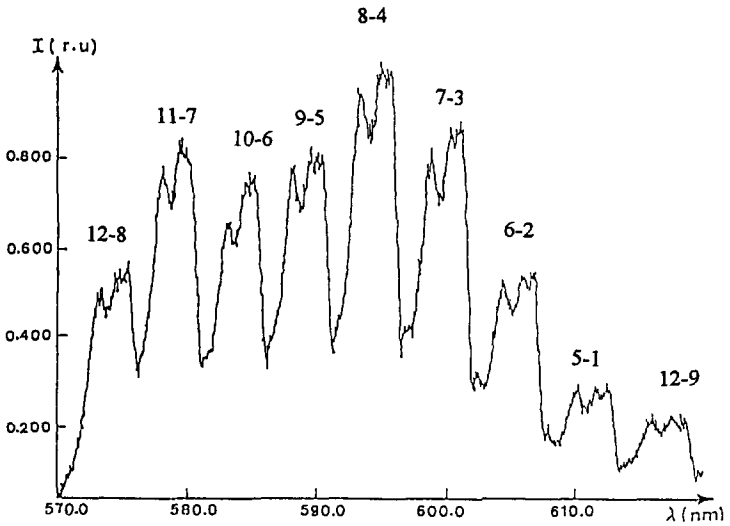

Fig. 3. — Same conditions as in figure 2 at $p = 0.4$ Torr and time $\Delta t = 2 \times 10^{-2}$ s (early afterglow).

that the (11-7) band is no longer dominant and that the vibrational bands $N_2(B, v' < 11)$ are well excited. The $[N_2(B, v')]$ vibrational densities are calculated in relative units from the following equation :

$$I_{BA}(v', v'') = \frac{C(\lambda) \cdot A_{v', v''}}{\lambda_{v', v''}} \cdot [N_2(B, v')] \tag{1}$$

where $C(\lambda)$ is the spectral response of the optical spectrometer, which has been calibrated by use of a tungsten lamp and $A_{v', v''}$ is the radiative emission probability [8]. The $[N_2(B, v')]$ vibrational distributions are reproduced in figure 4 for the Ar-10 % N_2 H.F. post-discharges at times $\Delta t = 5 \times 10^{-3}$ s-2×10^{-2} s and $p = 0.4$ Torr in (A) and at time $\Delta t = 0.3$ s and $p = 4.5$ Torr in (B). The curve (C) in figure 4 is deduced from the $N_2(B, v')$ densities published in reference [9] where the $N_2(B, v')$ states are mainly populated by the transfer of electronic energy from $N_2(A)$ to $N_2(X, v > 5)$ as :

$$N_2(A) + N_2(X, v > 5) \rightarrow N_2(X) + N_2(B, v') \tag{b}$$

with $k_b = (3 \pm 1.5) \times 10^{-11}$ cm^3/s [9].

The (A) (B) and (C) vibrational distributions in figure 4 have been normalized with $[N_2(B, 7)] = 3 \times 10^4$ cm^{-3} as reported in reference [9]. The $N_2(B, 11)$ peak dicreases, relatively to other $N_2(B, v')$, in going from the late to the early afterglow. The (B) distribution has been multiplied by 25 to be compared to the (A) distribution.

The shape of the (A) and (C) distributions are about the same as it concerns the disappearance of the $N_2(B, 11)$ maximum. Also it can be estimated that the present early afterglow at times $\Delta t = (0.5\text{-}2) \times 10^{-2}$ s is mainly produced by reaction (b). Consequently, the $N_2(B, v')$ densities can be written as :

$$[N_2(B, v')] = \frac{[N_2(A)] \cdot [N_2(X, v > 5)] \cdot k_b}{\nu^r_{v'} + [M_2] \cdot k_{Q, v'}} \tag{2}$$

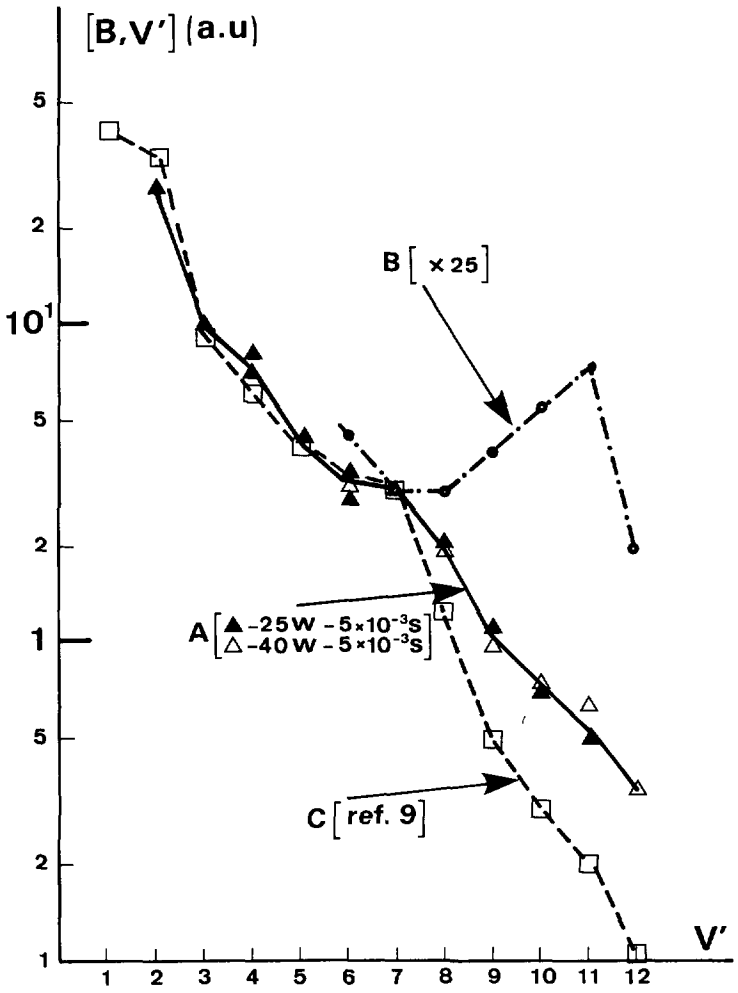

Fig. 4. — N_2, 1st pos. vibrational distributions in post-discharges A : early afterglow, Ar-10 % N_2, 0.4 Torr ; B : late afterglow, Ar-10 % N_2, 4.5 Torr and C : afterglow of a 60 W microwave discharge [9] (the two black triangles for $v' = 4$ and 6 are deduced from vibrational sequences $\Delta V = 2,3$ and $\Delta V = 3, 4$, respectively).

where the radiative frequency $\nu_{v'}^{r} = 1.5 \times 10^5\ s^{-1}$ [8] and the k_Q quenching rates by Ar, N_2, H_2 and CH_4 are (in cm^3/s) : 2×10^{-12} [2], 3×10^{-11} [2], 5×10^{-11} [10] and 3×10^{-10} [11], respectively.

The introduction of small densities of CH_4 in the N_2 D.C. post-discharge (0.5 Torr, 50 mA) leads to a decrease of $I_{BA}(v', v'')$ intensities without changing the $N_2(B, v')$ vibrational distribution as reproduced in figure 5a for bands at the origin of $N_2(B, v' = 2$ and 12). This decrease cannot be explained by the $N_2(B, v')$ quenching in equation (2) since $[CH_4] < 3 \times 10^{13}\ cm^{-3}$ and then $[CH_4]\, k_Q < 10^4\ s^{-1}$ is more than one order of magnitude lower than $\nu_{v'}^{r}$. The quenching of $N_2(A)$ and $N_2(X, v)$ by CH_4 is now considered :

$$N_2(A) + CH_4 \rightarrow \text{products} \qquad \text{(c)}$$

$$N_2(X, v > 5) + CH_4 \rightarrow \text{products}\,. \qquad \text{(d)}$$

One can derive that $N_2(B, v')$ is related to $N_2(A)$ and $N_2(X, v > 5)$ by :

$$[N_2(B, v')] = k(v') \cdot \exp - (\nu^A + k_c[CH_4])\,\Delta t \times \exp - (\nu^X + k_d[CH_4])\,\Delta t \qquad (3)$$

where $k(v') = \dfrac{[N_2(A)_0\ [N_2(X, v > 5)]]\,k_b}{\nu^r_{v'} + [M_2]\,k_{Q,v'}}$ The ν^A, ν^X frequencies represent the destructions, by reaction (b), by reaction with N atoms for $N_2(A)$ molecules and by diffusion on the tube wall (ν^A_w, ν^X_w).

- $\nu^A_w = \dfrac{(D_A p)}{\Lambda^2 p}$ (D_A diffusion coefficient of $N_2(A)$, $D_{Ap} = 160\ cm^3\ s^{-1}$ Torr [14] and Λ the diffusion length is $R/2.4$ for a tube of radius R).
- $\nu^X_w = \gamma_r \dfrac{\bar{V}}{2R}$, γ_r is the wall destruction probability of $N_2(X, v > 5)$ and $\bar{V}$ is the mean velocity of molecules [4].
- k_c and k_d are the quenching rates of reactions (c) and (d), respectively.

As a result of low k_d quenching rate : $k_d = 10^{-14}\ cm^3\ S^{-1}$ [11], it can be calculated that $\nu^X_w > k_d[CH_4]$ in equation (3) for $[CH_4] < 3 \times 10^{13}\ cm^{-3}$ and for $\gamma_r = 6 \times 10^{-4}$-$6 \times 10^{-3}$ as reported in references [15] and [16]. Also, equation (3) can be simplified as :

$$[N_2(B, v')] = k(v') \exp - (\nu^A + \nu^X + k_c[CH_4]\,\Delta t)\,. \qquad (4)$$

The k_c-rate coefficient can be determined from the slope of $I_{BA}(v', v'')$ in log unit *versus* CH_4 in figure 5a. From several experiments in N_2 and Ar-10 % N_2 D.C. and H.F. post-discharges, it has been obtained $k_c = 1.6(\pm 0.4) \times 10^{-12}\ cm^3/s$. Such a value is well related to $k_c[A, v' = 1, 2]$ published values : $k_c[A, v' = 1] = 1.2 \times 10^{-12}$ and $k_c[A, v' = 6] = 5.1 \times 10^{-12}\ cm^3/s$ [13], the $k_c[A, v' = 0]$ being largely lower : $k_c[A, v' = 0] = 3.2 \times 10^{-15}\ cm^3/s$ [12].

With H_2 in the N_2 D.C. and H.F. post-discharges, it was necessary to introduce higher quantity of H_2 to produce a signifiant decrease of I_{BA} as indicated in figure 5b for D.C. (0.5 Torr, 50 mA). The exponential decay is only obtained for $[H_2] > 10^{15}\ cm^{-3}$ where the $N_2(B, v')$ density is given by an equation which is similar to equation (3), as :

$$[N_2(B, v')] = k(v') \exp - (\nu^A + k_e[H_2])\,\Delta t \times \exp - (\nu^X + k_f[H_2])\,\Delta t \qquad (5)$$

where the $k_e$and k_f rate coefficients are for the following reactions :

$$N_2(A) + H_2 \rightarrow \text{products} \qquad (e)$$

$$N_2(X, v > 5) + H_2 \rightarrow \text{products}\,. \qquad (f)$$

In equation (5), $k(v')$ is decreasing with H_2 density as a result of $N_2(B, v')$ quenching (see Eq. (2)). This effect has been taken into account in the decay of $I_{B,A}$ in figure 5b. By taking the k_f published value : $k_f = 2 \times 10^{-15}\ cm^3/s$ [11], it has been determined a k_e-value of $4 \times 10^{-15}\ cm^3/s$. From several experimental sets in N_2 and Ar-10 % N_2 D.C. and H.F. post-discharges, the k_e-rate constants are in the 10^{-15}-$10^{-14}\ cm^3/s$ range. By comparing with the $k_e(A, v')$ published values : $k_e[A, v' = 0] \sim 2 \times 10^{-15}$, $k_e[A, v' = 1] = 4 \times 10^{-14}$ [12, 14], $k_e[A, v' = 2] = 6 \times 10^{-14}$ and $k_e[A, v' = 6] = 1 \times 10^{-12}\ cm^3/s$ [13], the k_e-values presently found indicate a quenching of $N_2(A, v' = 0, 1)$.

The initial sharp decay of I_{BA} observed in figure 5b could be the result of an increase of $\nu^A + \nu^X$ in equation (5). A sharp increase of N atom density in N_2 + (1-3 %) H_2 afterglow [16]

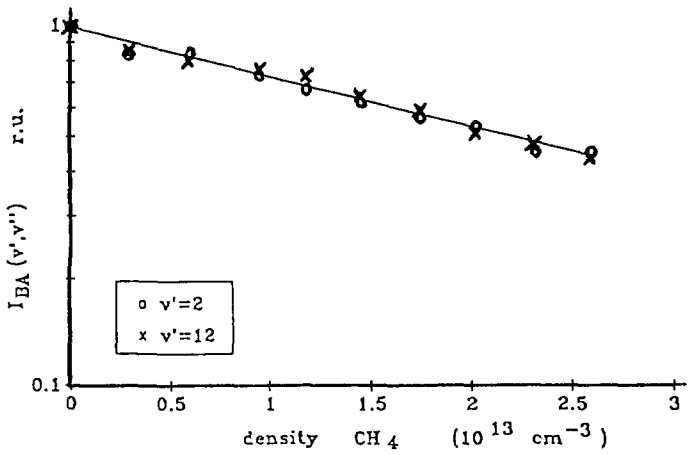

a)

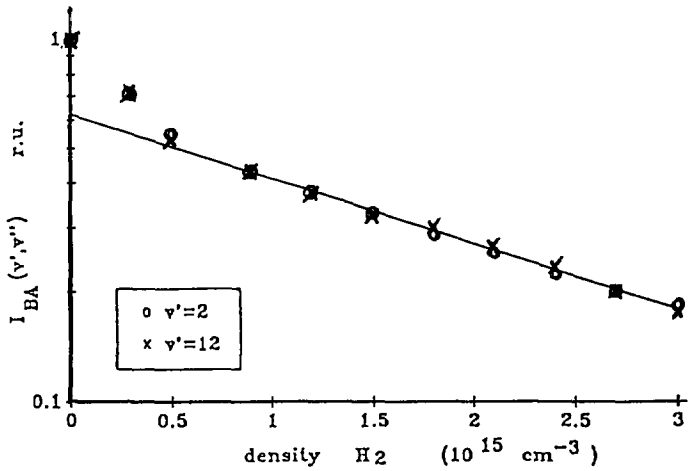

b)

Fig. 5. — N_2, 1st post relative intensities *versus* CH_4 (a) and H_2 (b) in D.C. N_2 post-discharge (0.5 Torr, 50 mA).

has been recently observed. This effect in the present early afterglow should increase ν^A by the $N_2(A) + N$ reaction.

5. Conclusion.

The kinetics reactions of active species in N_2 D.C. and H.F. post-discharges have been studied from emission spectroscopy. The late and early afterglows have been analysed in Ar-10 % N_2 at mean gas pressures of 4.5 and 0.4 Torr, respectively. In the 4.5 Torr late afterglow at time of 0.3 s, the N/N_2 dissociation degree was slighty higher after microwave discharges at 60 W, $R = 1$ cm (4.1 %) as compared to a positive column at $I = 50$ mA (~ 75 W), $R = 1$ cm (2.7 %).

An early afterglow has been detected in the range $(0.5\text{-}5) \times 10^{-2}$ s which mainly results from the excitation transfer: $N_2(A) + N_2(X, v > 5) \rightarrow N_2 + N_2(B, v')$. The addition of

CH_4 or H_2 in the N_2 post-discharge reduces the $N_2(B, v')$ production by quenching of $N_2(A)$ molecules. The $N_2(A) + (CH_4, H_2)$ quenching rates are $(1.6 \pm 0.4) \times 10^{-12}$ and 10^{-15}-10^{-14} cm^3/s respectively. By comparing with published values it is deduced that the $N_2(A, v')$ molecules are weakly excited in the D.C. and H.F. post-discharges at levels $v' < 2$.

References

[1] Ricard A., Oseguera J., Falk L., Michel H. and Gantois M., *IEEE Trans. Plasmas Sci.* **18** (1990) 940.

[2] Campbell I. M. and Thrush B. A., *Proc. Roy. Soc. A* **296** (1967) 201.

[3] Moisan M., Leprince P., Marec J., Zakzewski Z. *et al., IEE Conf. Pub.* **143** (1976) 382.

[4] Massabieaux B., Plain A., Ricard A., Capitelli M. and Gorse C., *J. Phys. B* **16** (1983) 1863.

[5] Malvos H., Ricard A., Moisan M. and Hubert J., *J. Phys. Colloq. France* **51** (1990) C 5-313.

[6] Ricard A., Malvos H., Bordeleau S. and Hubert J., ISPC-10, 201-12 (Bochum, 1991).

[7] Malvos H., Chave C., Ricard A., Michel H. and Gantois M., 2nd Nitriding/Carburizing Conf. (Cincinnati, 1989).

[8] Gilmore F. R., Laher R. R. and Espy P. J., *J. Phys. Chem. Ref. Data* **21** (1992) 1005.

[9] Piper L. G., *J. Chem. Phys.* **91** (1989) 864.

[10] Sperlein R. F. and Golde M. F., *J. Chem. Phys.* **89** (1988) 3113.

[11] Piper L. G., *J. Chem. Phys.* **97** (1992) 270.

[12] Slanger T. G., Wood B. J. and Black G., *J. Photochem.* **2** (1973) 63.

[13] Golde M. F., Ho G. H., Tao W. and Thomas J. M., *J. Phys. Chem.* **93** (1989) 1112.

[14] Levron D. and Phelps A. V., *J. Chem. Phys.* **69** (1978) 2260.

[15] Black G., Wise H., Schechter S. and Sharpless R. L., *J. Chem. Phys.* **60** (1974) 3526.

[16] Baravian G. and Ricard A., 11th ISPC (Loughborough 1993).